PROCEEDINGS OF SPIE

SPIEDigitalLibrary.org/conference-proceedings-of-spie

Optical trapping for tissue scaffold fabrication

Anna Linnenberger, Callie Fiedler, Justine J. Roberts, Stacey C. Skaalure, Stephanie J. Bryant, et al.

Anna Linnenberger, Callie Fiedler, Justine J. Roberts, Stacey C. Skaalure, Stephanie J. Bryant, Michael C. Cole, Robert R. McLeod, "Optical trapping for tissue scaffold fabrication," Proc. SPIE 8810, Optical Trapping and Optical Micromanipulation X, 88102F (12 September 2013); doi: 10.1117/12.2027869

SPIE.

Event: SPIE NanoScience + Engineering, 2013, San Diego, California, United States

Optical trapping for tissue scaffold fabrication

Anna Linnenberger,[1] Callie Fiedler,[1] Justine J. Roberts,[2] Stacey C. Skaalure,[2] Stephanie J. Bryant,[2,3] Michael C. Cole,[1] and Robert R. McLeod [1]

[1] Department of Electrical, Computer, and Energy Engineering, University of Colorado, 1111 Engineering Drive, 422 UCB, Boulder, CO 80309-0422, USA
[2] Department of Chemical and Biological Engineering, University of Colorado, 596 UCB Boulder, CO 80309-0596, USA
[3] Biofrontiers Institute, University of Colorado, 3415 Colorado Ave, Boulder, CO 80303, USA

ABSTRACT

We investigate holographic optical trapping combined with step-and-repeat maskless projection stereolithography for fine control of 3D position of living cells within a 3D microstructured hydrogel. C2C12 myoblast cells were chosen as a demonstration platform because their development into multinucleated myotubes requires linear arrangements of myoblasts. C2C12 cells are positioned in the monomer solution with multiple optical traps at 1064 nm and then are encapsulated by photopolymerization of monomer via projection of a 512x512 spatial light modulator (SLM) illuminated at 405 nm. High 405 nm sensitivity and complete insensitivity to 1064 nm is enabled by a lithium acylphosphinate (LAP) salt photoinitiator. Use of a polyethylene glycol dimethacrylate (PEGDMA) based monomer is compared to that of polyethylene glycol (PEG) hydrogels formed by thiol-ene photo-click chemistry for patterning structures with cellular resolution, and for maintaining cell viability. Cells patterned in thiol-ene with RGD are shown to retain viability up to 4 days after the trapping and encapsulation procedure. Further, cells patterned in thiol-ene with RGD and a degradable ester link, are shown to fuse, indicating the initial stages of development of multi-nucleated cells.

Keywords: Tissue Engineering, Optical Trapping, spatial light modulators (SLMs), micro-stereolithography

1. INTRODUCTION

Crosslinked polymers are often utilized to create synthetic hydrogel scaffolds for tissue engineering by encapsulating living cells whose development is studied to answer fundamental biological questions and to fabricate regenerative medical implants. Current approaches for fabricating these hydrogel constructs do not provide simultaneous 3D control of polymer structure and 3D placement of cells. 2D patterning of cells is commonly accomplished by lithographic deposition of an extra-cellular protein, for example poly-L-lysine is used to direct neuronal cell attachment and growth on planar electrode arrays [1,2,3]. Unfortunately, 2D structures do not accurately represent living tissue and thus are not appropriate for many basic biological studies or tissue engineering therapies. As a result, a variety of methods to construct complex 3D tissue scaffolds are under study, most derived from 3D printing [4]. While these methods result in 3D structures that define scaffold shape, they provide no control over the internal distribution of cells within the scaffold. The random distribution of cells limits the repeatability of studies and makes precise experiments involving cell-cell interaction impossible in a 3D scaffold environment. Alternatively, optical trapping has been used to precisely arrange living bacteria in a polymerizable solution [5]. However, the depth of a high-NA optical trapping system is limited by aberrations [6] to approximately ± 20 μm and thus does not provide true 3D structuring of cells.

In this article, we investigate the use of holographic optical trapping, to precisely arrange cells within layers, in combination with projection stereolithography, to fabricate multilayered 3D structures encapsulating these cells. Cells are first arranged by optical traps in a liquid monomer mixture which is then locally crosslinked into a hydrogel by photopolymerization to permanently entrap the cells. The sample is translated laterally and the process is repeated to

Optical Trapping and Optical Micromanipulation X, edited by Kishan Dholakia, Gabriel C. Spalding,
Proc. of SPIE Vol. 8810, 88102F · © 2013 SPIE · CCC code: 0277-786X/13/$18 · doi: 10.1117/12.2027869

pattern arbitrarily large *x,y* dimensions. The finished layer is then moved away from the cover slip, causing inflow of the fresh cells and monomer which will be formed into the next layer. Live cell lithography [5] thus provides micron-scale 3D control of both cellular distribution and gel structure to enable new forms of engineered 3D live cell tissue scaffolds [7].

To illustrate the potential of this approach for complex 3D structuring of micron-scale objects within a hydrogel, we first demonstrate arrangement of silica beads encapsulated in multiple depth layers and multiple lateral steps. To further demonstrate applicability to cellular biology, we structure C2C12 skeletal myoblasts in biologically relevant patterns including a multi-layer hydrogel with linear arrangements of viable C2C12 cells. This work provides a foundation for future studies of myotube formation via cellular junctions, and eventually formation of complex hierarchical tissue structures.

2. FABRICATION SYSTEM

A diagram of the Cube (Boulder Nonlinear Systems) holographic optical trapping instrument is shown in Fig. 1 [8]. Diffraction limited optical traps are formed using a 10 watt 1064 nm fiber laser (YLR-5-1064-LP, IPG Photonics) which illuminates a mirrored 512x512 pixel phase-only liquid crystal SLM (P512-1064 SLM, Boulder Nonlinear Systems) through a Keplerian beam expander. The phase patterns on the SLM are computed using the Lenses and Gratings algorithm [9,10] programmed in OpenGL and running on a graphics co-processor (Quadro FX 5600, nVidia). The SLM is imaged to the back aperture of the 1.35 NA oil immersion microscope objective (UAPON 40XO340, Olympus) through a 4F imaging system. The field of view of the microscope objective is 550 mm, but the intermediate image of the sample is magnified such that the sample area and the area over which the SLM can efficiently optically trap are more closely matched. Thus, the microscope images 120 μm x 90 μm within the sample. The objective has at least 70% transmission from 405 nm to 1064 nm, making it possible to optically trap, image, and photopolymerize the sample simultaneously. This system is capable of simultaneously trapping up to 400 objects within a volume whose depth is limited by aberrations to approximately ±20 μm [5] without time sharing, in addition to correcting for aberrations as a result of the SLM and optical train [9].

A 410 mW, 405 nm LED (M405L2, Thorlabs) is used as the light source to provide spatially uniform illumination with low coherence to suppress speckle noise and interference. The LED is polarized and used to illuminate a 512x512 pixel liquid crystal SLM (P512-532, Boulder Nonlinear Systems) employed as a programmable amplitude mask. In contrast to the SLM used for trapping, the linear polarization incident upon this SLM is oriented at 45 degrees relative to the liquid crystal director, resulting in a pixilated programmable polarization rotation. This polarization rotation is converted to amplitude modulation by an orthogonal polarizer. These crossed polarizers prevent unwanted reflections off of surfaces of the SLM from degrading the quality of the off state, resulting in a contrast ratio of 200:1 or better. A dichroic mirror (NT69-201, Edmund Optics) is used to introduce the 405 nm pattern into the imaging arm of the Cube, as shown in Fig. 2, such that the SLM plane is in focus at the sample. The imaging system de-magnifies the pixel pitch from 15 μm at the SLM to 0.67 μm at the sample.

This system is capable of photopolymerizing hydrogel patterns with approximately 10 μm resolution in 1-5 seconds using a sample plane intensity of up to 70 mW/cm^2. This resolution is material-limited due to the balance of the polymerization reaction and the diffusion of photo-generated species in the initially liquid solution. We note that, unlike the 1064 nm trapping pathway, possible aberrations of the 405 nm optical imaging path were not measured or corrected because polymer feature resolution at the diffraction limit is not required for creating structures matching cellular resolution. A critical feature of the gelation process is that it must not perturb the position of objects held in the 1064 nm traps. High intensity in a single spot, such as that from a focused 405 nm laser, gels the polymer more quickly but completely disrupts the positions of trapped objects as polymerization shrinkage and diffusional mass transport overcome the approximately pN trap strength.

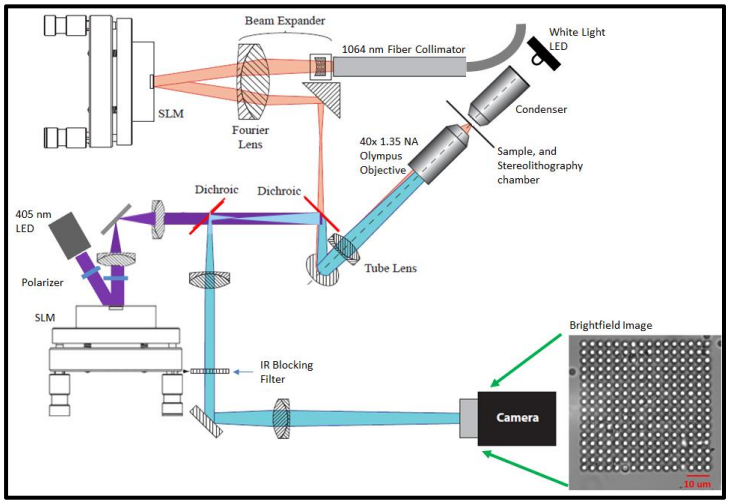

Figure 1 Tissue Scaffold Manufacturing System

Large 3D scaffolds containing precisely positioned cells can be built from many individual layers through additive manufacturing [11]. In traditional stereolithography [12], multi-layer photopolymerized structures are formed by spreading a thin monomer layer onto a base plate using a blade. The thin monomer layer is exposed to the curing source to selectively photopolymerize regions within the layer. The structure is lowered, and a new thin layer of monomer is spread across the part. The process is repeated enabling fabrication of thick 3D structures. An alternative, which removes the open surface and applicator blade, is to hold the thin monomer layer between the part and an optical window whose inner surface has been coated to prevent adhesion of polymer [13]. As we show in Fig. 2, this approach has the particular advantage that the entire device can be miniaturized sufficiently to fit into the slide holder of an *x,y* motorized microscope stage. The lower surface is a standard coverslip whose upper surface is silane coated to prevent bonding of monomer during polymerization. The coating is deposited on the coverslip by mixing 0.6 g IPA with 0.017 g acetic acid (A6268, Aldrich) and 0.04 g (heptadecafluoro1.1.2.2-tetra-hydrodecyl) trimethoxy silane (Gelest). The mixture is placed between two coverslips stacked together, and the coverslips are baked on a hot plate at 70 ºC for 10 minutes. After baking coverslips are detached from each other, and rinsed with isopropyl alcohol and distilled water. The top of the fabrication chamber is formed by a microscope slide and a glass spacer treated with a siloxane adhesion promoter. The coating procedure is similar to that of the coverslip; however, 3-(triethoxysilyl)propyl methacrylate (Tokyo Chemical Industry) is used in place of (heptadecafluoro1.1.2.2-tetra-hydrodecyl) trimethoxy silane. The all-glass construction enables brightfield illumination to enter the chamber from above (Luxeon III Star, MR-WC100-20S). The objective working distance enables cells to be trapped and polymerization to be initiated up to 40 μm from the inner surface of the window. The cover slip window is held in a baseplate attached to the *x,y* translation stages (MS-2000-XY, ASI) of the Cube.

A thin fluid layer is initially formed between the top and bottom windows by adjusting the *z* actuators (here manual screws, although the design is compatible with miniature motorized actuators). The glass spacer compensates for the mechanical height of the chamber, allowing the first layer to be near zero thickness. After a layer of cells encapsulated in a structured hydrogel is formed, the *z* actuators are used to raise both the upper window and the adhered gel layer, after which the process repeats. Scaffolds with 100 μm layers and heights of approximately 2 mm have been fabricated, as shown in Fig. 3. The minimum layer thickness of several microns is determined by the actuator resolution and the cell diameter while the maximum sample thickness of several cm is limited by actuator range and the sample volume of the microscope. Individual layer thickness can be optically verified using the motorized *z* autofocus actuator on the objective. The result is a precise arrangement of cells with fine control of 3D position within each layer, and extended

3D position throughout the multi-layer scaffold. Layers with different cell types [5] and cell distributions can be sequentially added to rapidly fabricate complex scaffold geometries precisely loaded with individual cells.

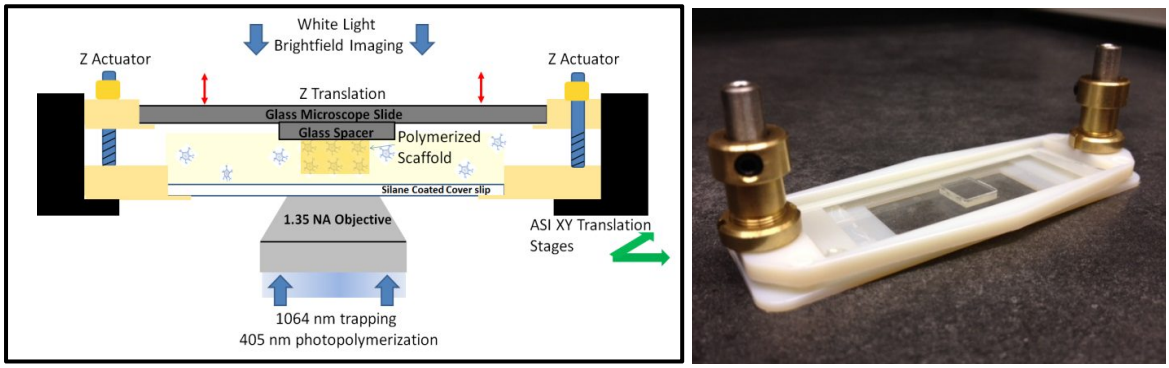

Figure 2 (left) Diagram of the micro-stereolithography system placed in the sample chamber (right) actual system

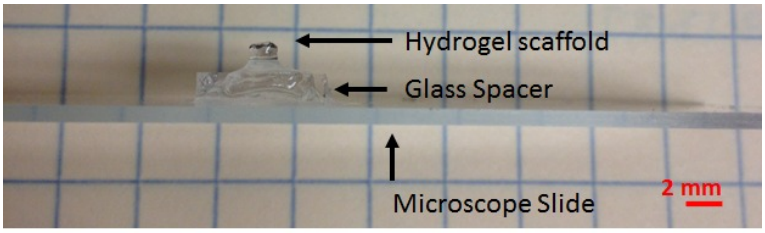

Figure 3 Sample hydrogel structure fabricated through additive layering. 100 um layers are sequentially cured to form a 2 mm hydrogel scaffold

3. MATERIALS

Hydrogels are crosslinked polymers, which are often utilized to create scaffolds for cells. Poly (ethylene glycol) diacrylate (PEGDMA), which cross-links though a free radical mediated chain growth, is a common platform for encapsulation of cells. It is a semipermeable hydrogel that can be designed to biodegrade, has a tunable modulus, and is generally considered biocompatible. However, acrylate systems that photopolymerize through chain growth cannot be propagated by oxygen radicals, and therefore there are more oxygen radicals that can be damaging to cells [14]. Alternatively, recent research has focused on encapsulation of cells within thiol-ene photopolymerized PEG peptide hydrogels for studies of: 3D cell biology [15,16], the controlled release of therapeutically relevant proteins [17], directing stem cell differentiation [18], and promoting tissue regeneration [19]. Thiol-ene systems can be propagated by oxygen radicals, thus reducing the number of oxygen radicals present that can damage cells. In this work multiple monomer solutions are evaluated to quantify the resolution and repeatability of the structures that can be fabricated and viability of cells encapsulated within the hydrogel.

The first monomer solution consists of 49.9 wt. % phosphate buffered saline (PBS, Cellgro), 0.1 wt. % lithium phenyl-2,4,6-trimethylbenzoylphosphinate (LAP photoinitiator) [20], 10 wt % poly(ethylene glycol) dimethacrylate [21] (PEGDMA, Sigma), and 40 wt. % cell solution. The cell solution consists of $0.5x10^6$ C2C12 cells/mL suspended in growth media. The growth media consists of high glucose Dulbecco's Modified Eagle's Medium containing 10% fetal bovine serum, 1% Penicillin/Streptomyocin, 0.5 µg/mL fungizone. This monomer is henceforth referred to as the 10 wt % PEGDMA monomer.

To increase viscosity, and thus limit out-diffusion of oligomers when patterning scaffolds, a secondary PEGDMA monomer solution consisting of 49.9 wt. % PBS, 0.1 wt. % LAP initiator, 30 wt. % PEGDMA, and 20 wt. % cell solution is also considered. The increased viscosity of the monomer enables cells to remain suspended as opposed to settling to the coverslip. The latter reduces the number of cells available for trapping, necessitating an increase in cell

density to $2x10^6$ C2C12 cells/mL suspended in growth media. This monomer is henceforth referred to as the 30 wt. % PEGDMA monomer.

Degradable and non-degradable thiol-ene hydrogels were likewise considered. The non-degradable thiol-ene hydrogel consists of C2C12 cells suspended, at a density of $1x10^6$ cells/mL, in a stoichiometrically balanced (1 ene to 1 thiol) monomer solution comprised of 10 wt. % 4-arm PEG-norbornene [22] dissolved in PBS, 0.05 wt. % LAP photoinitiator, 4 wt. % PEG-dithiol, and 0.135 wt. % CRGDS. The degradable thiol-ene hydrogel consists of C2C12 cells suspended, at a density of $1x10^6$ cells/mL, in a monomer solution comprised of 10 wt. % 4-arm PEG-norbornene with an ester link dissolved in PBS, 0.05 wt. % LAP photoinitiator, 3.2 wt. % PEG-dithiol, and 0.135 wt. % CRGDS. The degradable thiol-ene has a stoichiometric ratio of 0.8 to reduce the cross-linking density, and increase the rate at which the hydrogel degrades.

LAP was chosen over initiators commonly used for tissue engineering such as I2959 or eosin [23,24,25] for several reasons. First, its high water solubility (up to 8.5 wt%) enables photosensitivity to be adjusted over a large range. Second, LAP exhibits low yellowing making it possible to deliver the brightfield illumination through a thick layer of polymerized scaffold without significant absorption. The use of 405 nm, rather than the common 365 nm, reduces cytotoxicity [20] of repeated exposures during multi-layer fabrication and also enables the use of a high-power LED module for faster fabrication. This same choice also significantly relaxes the bandwidth requirements on the microscope objective which must extend up to 1064 nm. Finally, LAP, in the formulation here, did not initiate polymerization in solution when exposed to approximately 0.03 GW/cm^2 of 1064 nm trapping for 10 minutes.

Structures containing both two micron silica beads (Sekisui) and live cell structures are fabricated. The live cells used here are C2C12 mouse myoblast (ATCC) cultured in growth medium (as above), at 37°C and in 5% CO_2. Upon reaching 70-80% confluency, cells were passaged with 0.25% trypsin, and either re-plated for continued expansion or combined with polymer solution for photoencapsulation. After entrapment within scaffolds and incubating for multiple days, cells are assessed for viability with the LIVE/DEAD® membrane integrity assay, and imaged with a confocal laser scanning microscope (CLSM, Zeiss LSM 510, Thornwood, NY) at 40x magnification. Cells tested for viability are incubated in growth media consisting of high glucose Dulbecco's Modified Eagle's Medium containing 10% fetal bovine serum, 1% Penicillin/Streptomyocin, 0.5 μg/mL fungizone. In cell differentiation tests, the fetal bovine serum in the growth media is replaced with horse serum.

4. RESULTS

4.1 Hydrogel patterning

Patterning of hydrogel structures that contain organized arrangements of 2 μm silica beads demonstrates the ability to merge optical trapping with micro-stereolithography, and is used to verify that optical traps are sufficiently strong to hold objects in place while the surrounding monomer is cured. Fig. 4a and 4b illustrate multi-layer grids patterned with 2 μm silica beads suspended in 10 wt% PEGDMA monomer. Polymer voxels several hundred microns in diameter are fabricated to encase each layer. The layers each contain a 6x6 grid of silica beads, and each grid is separated by 95 μm. Registration between layers is maintained to within 4 μm. A drawing of the multi-layer structure is shown in Fig. 4c to demonstrate scale.

To demonstrate that the maskless lithography system is capable of high resolution hydrogel structuring a much smaller arrangement of 2 μm silica beads is assembled through a series of 4 exposures (Fig. 4d). The first exposure encased 4 beads in a polymer voxel approximately 6 – 10 μm in diameter, denoted in the figure with a dashed line. The second exposure encased a single bead, the third exposure encased 4 more beads, and the last exposure encased a single bead. The very weak difference in index of refraction between the polymerized voxel and liquid monomer prevents the ability to directly image structures using differential interference contrast imaging. Thus, to map the polymerized region trapped beads are used as probes to trace out the edge of the polymer voxel such that approximate dimensions can be determined.

Although the index difference is weak, the hydrogel structures are sufficiently strong to support cells and beads for multi-day experiments.

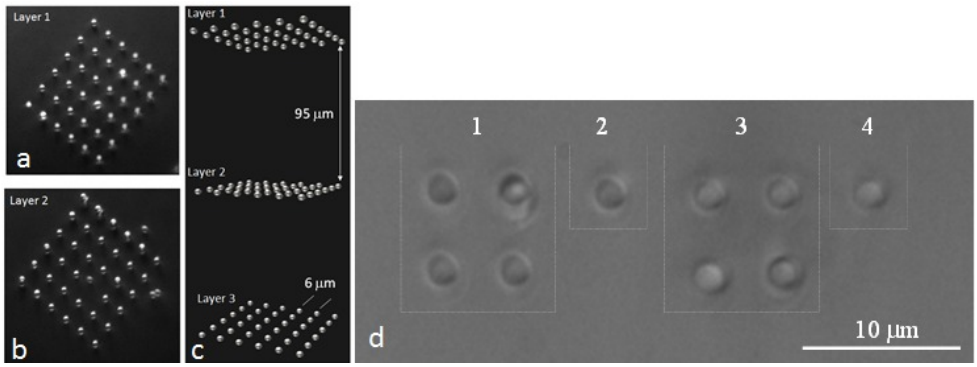

Figure 4 Demonstration of optically trapped beads patterned into grids, and photopolymerized into polymer voxels. (a,b) DIC images of two layers of arranged 2 µm silica beads are shown. (c) An illustration of the patterned structure is shown to demonstrate scale (d) DIC image after four sequential "step and repeat" patterning steps. In each exposure, the 2 µm beads are first trapped at 1064 nm, then the surrounding liquid is locally gelled using 405 nm light controlled by the SLM. The material patterning resolution is demonstrated by the bead spacing while the stability of the traps during gelation is demonstrated by the regular grid.

The primary disadvantage of patterning structures with a 10 wt. % PEGDMA monomer is the low viscosity. As the liquid monomer is exposed to the curing source, oligomers form and rapidly diffuse into the surrounding monomer, limiting structure resolution. In order to pattern structures with cellular resolution, it is necessary to optically pre-cure a large area to just below the gel point, followed by a patterned exposure which locally causes gelation. In this work an area of 340 µm x 340 µm is illuminated in the pre-cure, followed by illumination of 11 µm x 11 µm regions in the secondary exposure.

Use of a pre-cure enables pattering of structures with cellular resolution; however, the outflow and accumulation of oligomers influences the scale of polymer voxels in subsequent cures. Use of a higher viscosity, 30 wt. % PEGDMA monomer reduces this problem, but still makes patterning of structures with a consistent size challenging. As can be seen in Fig 5, a pre-cure of 2000 ms at 70 mW/cm^2 followed by a patterned exposure of varying duration and power resulted in polymer voxels approximately equal in diameter in cures 1 through 5. However, in cure 6 the oligomer concentration in the surrounding monomer was sufficiently high that the radius of the polymer voxel patterned is approximately 4 times greater than that of cures 1 through 5. To avoid this problem, fresh monomer can be injected into the sample after each cure. However, this is an inefficient use of materials.

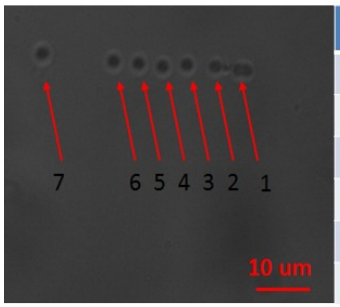

Bead	Cure	Voxel Radius
1	150 ms at 21 mW/cm^2	3 µm
2	50 ms at 3.5 mW/cm^2	3 µm
3	50 ms at 3.5 mW/cm^2	2 µm
4	50 ms at 3.5 mW/cm^2	2 µm
5	50 ms at 3.5 mW/cm^2	2 µm
6	50 ms at 3.5 mW/cm^2	8 µm

Figure 5 Out-diffusion of oligomers generated when patterning PEGDMA monomer make it challenging to pattern polymer voxels of a consistent diameter. (left) 2 µm silica beads are sequentially encapsulated in polymer voxels of 30 wt% PEGDMA monomer. After a bead is encapsulated, a new bead is trapped and translated until it is sitting adjacent to the edge of the previously fabricated polymer voxel. Thus, the position of the beads marks the approximate radius of the previously cured polymer voxel. Polymer voxels from cures 1 through 5 are all approximately 4-6 µm in diameter. However, cure 6 resulted in a significantly larger polymer voxel, as can be seen by the position of bead 7. (right) curing conditions and resulting voxel radius

In order to maintain an efficient use of materials, and pattern hydrogel features of consistent size, one option is to consider alternative monomers that polymerize through step-growth as opposed to chain-growth. Thiol-ene with LAP as a photoinitiator is a highly sensitive monomer that can be used to pattern structures with cellular resolution without requiring a pre-cure. Furthermore, the polymer structures are sufficiently strong to enable rinsing after pattering such that the structures can be imaged within the Cube using brightfield imaging. A series of polymer voxels just over 10 µm in diameter are shown in Fig. 6. The area of exposure is marked with a red dashed line. In each of the 7 cures shown below the liquid monomer is exposed to the curing source for 700 ms, with an incident power of 56 mW/cm^2. As can be seen cure 1 and cure 2 do not fully form into the desired polymer structures. However, cures 3 through 7 result in polymer voxels of a fairly consistent diameter. This indicates that out diffusion of oligomers is still occurring, but the consistency in the diameter of the polymerized feature indicates significantly reduced oligomer outflow as compared to PEGDMA.

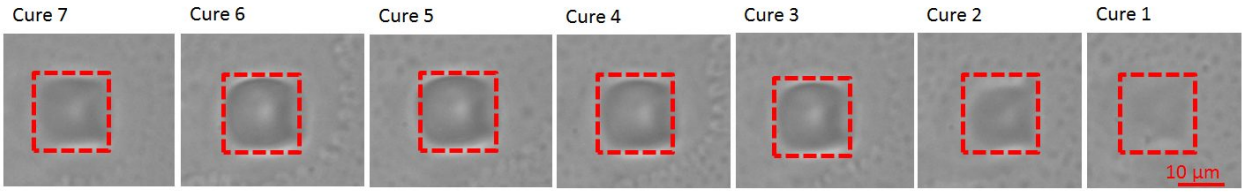

Figure 6 Patterning of sequential 10 µm voxels of thiol-ene polymer separated by 200 microns. The time between exposures is several seconds to allow time to translate the sample. Structures are patterned with no pre-cure, illustrating greater spatial control and reduced oligomer out-diffusion.

4.2 Cell Viability Testing

Multiple samples of C2C12 cells are encased within polymer voxels of: 10 wt. % PEGDMA modified with the cell adhesion peptide RGD, thiol-ene, and thiol-ene modified with RGD. During the patterning and encapsulation process cells are not exposed to the trapping source for more than 1 minute, and the power per trap is less than 200 mW. Optical trapping under these conditions has been shown to retain cell viability [26]. After entrapment samples are immediately incubated at 37 °C and in 5% CO_2 for multiple days. Growth media is replaced every 2 days. After incubation cells are assessed for viability with the LIVE/DEAD® membrane integrity assay, and imaged with a confocal laser scanning microscope. Fig 7 shows one of several Live/Dead assays completed with 10 wt. % PEGDMA modified with RGD. Green fluorescence indicates a healthy cell membrane. After 48 hours cells patterned in PEGDMA modified with RGD show minimal viability.

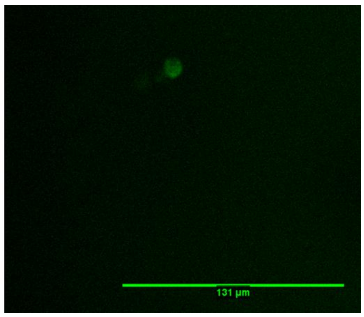

Figure 7 Live/Dead Assay of cells optically trapped and encapsulated within PEGDMA modified with RGD. Assay was completed 48 hours after encapsulation, and resulted in minimal viability.

Fig. 8 shows one of several Live/Dead assays of cells encapsulated within thiol-ene modified with RGD. Samples were tested 4 days after encapsulation. When RGD is not used cells show greater viability than samples patterned with PEGDMA, but not all cells encapsulated are viable. When RGD is used, as shown in Fig. 8, the vertical line of three cells retain viability, and look equally healthy as compared to the surrounding cells that were not exposed to the optical trapping source.

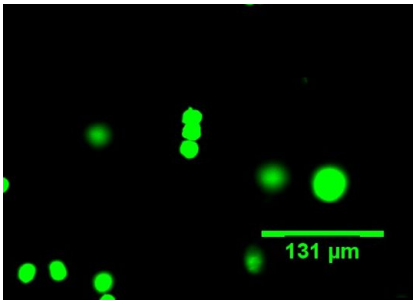

Figure 8 Live/Dead Assay of cells encapsulated in thiol-ene after 4 day incubation. The vertical line of 3 cells is arranged with optical trapping, and surrounding cells are not optically trapped. All cells contained within the hydrogel voxel are viable.

4.3 Cell Fusion

To show the potential to use optical trapping in combination with micro-stereolithography to fabricate multi-nucleated cells, C2C12 cells are arrange into lines and are encapsulated in the degradable thiol-ene modified with RGD. The samples are incubated for 4 days in differentiation media. A brightfield image of a line of 4 cells that has begun to fuse, which is necessary to forming a single multi-nucleated cell, is shown in Fig. 9.

Figure 9 Brightfield image of a line of 4 cells that were patterned to form a line, and encapsulated in thiol-ene hydrogel with RGD. Cells were incubated in growth media with 10% horse serum. After 4 days cells began to fuse, showing the very beginning stages of formation of a multi-nucleated cell.

5. CONCLUSIONS

In this work we demonstrate a system that merges holographic optical trapping with micro-stereolithography to pattern C2C12 cells in a hydrogel. Multiple monomer solutions were evaluated for their ability to pattern structures with cellular resolution, and for maintaining cell viability. This work demonstrates that 10 wt. % and 30 wt. % PEGDMA monomers can be used to pattern hydrogel features with diameters of 6 - 10 µm; however, rapid out diffusion of oligomers make patterning a series polymer voxels with a consistent diameter challenging. By making use of step-growth as opposed to chain-growth for photopolymerization, thiol-ene with LAP as a photoinitiator removed the need to pre-cure, and resulted in more consistent feature dimensions.

Multiple Live/Dead assays were completed with cells patterned in PEGDMA modified with the cell adhesion peptide RGD, thiol-ene, and thiol-ene modified with RGD. After 48 hours samples encapsulated within PEGDMA modified with RGD show minimal viability. Cells encapsulated in thiol-ene without RGD that are incubated for 4 days showed improved viability over that of PEGDMA. Maximum viability is seen when cells are patterned in thiol-ene with RGD. Cells encapsulated in a degradable thiol-ene with RGD that are incubated in growth media with 10% horse serum are shown to fuse within 4 days, indicating differentiation that could lead to the formation of a multi-nucleated cell.

ACKNOWLEGEMENTS

The authors would like to acknowledge the support of: NSF GOALI (ECCS 0954202), NSF CAREER (ECCS 0847390), Air Force MURI FA9550-09-1-0677, NSF GRFP, NIST MSE Fellowship, Teets Family Endowed Doctoral Fellowship, and a University of Colorado Innovative Seed Grant, which made this research possible.

REFERENCES CITED

[1] James, C. D., Davis, R., Meyer, Turner, M.A., Turner, S., Withers, G., Kam, L., Banker, G., Craighead, H., Isaacson, M., Turner, J., and Shain, W. "Aligned microcontact printing of micrometer-scale poly-L-lysine structures for controlled growth of cultured neurons on planar microelectrode arrays," IEEE Trans. Biomed. Eng. 47, 17-21(2000).

[2] Jun, S.B., Hynd, M. R., Dowell-Mesfin, N., Smith, K.L., Turner, J. N., Shain, W., and Kim, S.J. "Low-density neuronal networks cultured using patterned poly-l-lysine on microelectrode arrays," J. of Neurosci. Methods 160, 317-326 (2007).

[3] Branch, D. W., Wheeler, B. C., Brewer, G. J., and Leckband, D. E. "Long-term maintenance of patterns of hippocampal pyramidal cells on substrates of polyethylene glycol and microstamped polylysine," IEEE Trans. Biomed Eng. 47, 290-300 (2000).

[4] Tsang, V. L., and Bhatia, S. N. "Three-dimensional tissue fabrication," Adv. Drug Deliv. Rev 56, 1635-1647 (2004).

[5] Mirsaidov, U., Scrimgeour, J., Timp, W., Beck, K., Mir, M., Matsudaira, P., and Timp, G. "Live cell lithography: using optical tweezers to create synthetic tissue," Lab Chip 8, 2174-2181 (2008).

[6] Sinclair, G., Jordan, P., Leach, J., Padgett, M. J., and Cooper, J. "Defining the trapping limits of holographical optical tweezers," J. Mod. Opt. 51, 409-414 (2004).

[7] Nguyen, K. T., and West, J. L. "Photopolymerizable hydrogels for tissue engineering applications," Biomaterials 23, 4307-4314 (2002).

[8] Gibson, G.M., Bowman, R.W., Linnenberger, A., Dienerowitz, M., Phillips, D.B., Carberry, D.M., Miles, M.J., and Padgett, M.J. "A compact holographic optical tweezers instrument," Rev. Sci. Instrum. 83, 113107-113107 (2012).

[9] Liesener, J., Reicherter, M., Haist, T., and Tiziani, H. J. "Multi-functional optical tweezers using computer-generated holograms," Opt. Commun. 185, 77-82 (2000).

[10] Sinclair, G., Leach, J., Jordan, P., Gibson, G., Yao, E., Laczik, Z., Padgett, M., and Courtial, J. "Interactive application in holographic optical tweezers of a multi-plane Gerchberg-Saxton algorithm for three-dimensional light shaping," Opt. Express 12, 1665-1670 (2004).

[11] Linnenberger, A., Bodine, M., Fiedler, C., Roberts, J., Skaalure, S., Quinn, J., Bryant, S., Cole, M., and McLeod, R., "Three dimensional live cell lithography," Opt. Express 21, 10269-10277 (2013).

[12] Sun, C., Fang, N., Wu, D.M., and Zhang, X. "Projection micro-stereolithography using digital micro-mirror dynamic mask," Sensor Actuat. A-Phys 121, 113-120 (2005).

[13] Gauvin, R., Chen, Y. C., Lee, J.W., Soman, P., Zorlutuna, P., Nichol, J. W., Bae, H., Chen, S., and Khademhosseini, A., "Microfabrication of complex porous tissue engineering scaffolds using 3D projection stereolithography," Biomaterials 33(15), 3824–3834 (2012).

[14] Lin, C., Raza, A., Shih, H., "PEG hydrogels formed by thiol-ene photo-click chemistry and their effect on the formation and recovery of insulin-secreting cell spheroids," Biomaterials 32(36), 9685-9695 (2011).

[15] Schwartz, M.P., Fairbanks, B.D., Rogers, R.E., Rangarajan, R, Zaman, M.H., Anseth, K.S., "A synthetic strategy for mimicking the extracellular matrix provides new insight about tumor cell migration," Integr. Biol.2, 32–40 (2010).

[16] Benton, J.A., Fairbanks, B.D., Anseth, K.S., "Characterization of valvular interstitial cell function in three dimensional matrix metalloproteinase degradable PEG hydrogels," Biomaterials 30, 6593– 6603 (2009).

[17] Aimetti, A.A., Machen, A.J., Anseth, K.S. "Poly(ethylene glycol) hydrogels formed by thiol-ene photopolymerization for enzyme-responsive protein delivery," Biomaterials 30, 6048–6054 (2009).

[18] Anderson, S.B., Lin, C.C., Kuntzler, D.V., Anseth, K.S., "The performance of human mesenchymal stem cells encapsulated in cell-degradable polymer-peptide hydrogels," Biomaterials 32, 3564– 3574 (2011).

[19] Terella, A., Mariner, P., Brown, N., Anseth, K., Streubel, S.O., “Repair of a calvarial defect with biofactor and stem cell-embedded polyethylene glycol scaffold,” Arch. Facial Plast. Surg. 12, 166–171(2010).
[20] Fairbanks, B.D., Schwartz, M.P., Bowman, C.N., Anseth, K.S., “Photoinitiated polymerization of PEGdiacrylate with lithium phenyl-2,4,6-trimethylbenzoylphosphinate: Polymerization rate and cytocompatibility,” Biomaterials 30, 6702–6707 (2009).
[21] Sawhney, A. S., Pathak C. P., and Hubbell, J.A., "Bioerodible hydrogels based on photopolymerized poly (ethylene glycol)-co-poly (. alpha.-hydroxy acid) diacrylate macromers." Macromolecules 26(4), 581-587 (1993).
[22] Fairbanks, B.D., Schwartz, M.P., Halevi, A.E., Nuttelman, C.R., Bowman, C.N., Anseth, K.S., “A versatile synthetic extracellular matrix mimic via thiol-norbornene photopolymerization,” Adv. Mater. 21, 5005–5010 (2009).
[23] Bryant, S. J., Nuttelman, C. R., and Anseth, K. S., "Cytocompatibility of UV and visible light photoinitiating systems on cultured NIH/3T3 fibroblasts in vitro." J. of Biomaterials Science, Polymer Edition 11(5), 439-457 (2000).
[24] Williams, C.G., Malik, A.N., Kim, T.K., Manson, P. N., and Elisseeff, J. H., "Variable cytocompatibility of six cell lines with photoinitiators used for polymerizing hydrogels and cell encapsulation." Biomaterials 26(11), 1211-1218 (2005).
[25] Fedorovich, N. E., Oudshoorn, M. H., van Geemen D., Hennink, W. E., Alblas, J., and Dhert, W.J.A., "The effect of photopolymerization on stem cells embedded in hydrogels." Biomaterials 30(3), 344-353 (2009).
[26] Liang, H., Vu, K.T., Krishnan, P., Trang, T.C., Shin, D., Kimel, S., and Berns, M.W. "Wavelength dependence of cell cloning efficiency after optical trapping," Biophysical journal 70, 1529-1533 (1996).